Diagnosis of the Technical Condition of High-tech Complexes by Probabilistic Methods

V. Budashko, A. Sandler & V. Shevchenko
National University "Odessa Maritime Academy", Odessa, Ukraine

ABSTRACT: When designing multilevel systems for monitoring the parameters and characteristics of high-tech complexes, it is necessary to effectively control the state of the elements of generating units. Existing control systems for their specification and technical characteristics do not fully meet the monitoring objectives. The capabilities of existing known systems have limitations on the depth of use and compensation for the impact of operational factors. The article proposes and substantiates the feasibility of using the principle of automated measurement and control of load in high-tech complexes based on the probabilistic approach. It is established that the presence of errors in the means of measurement and control leads to specific errors that should be taken when assessing the quality of control, solving management and control tasks. To register the transition of parameters beyond the limit values, a new sensor circuitry based on fiber-optic elements is proposed. The main difference of the proposed diagnostic tool is the invariance to operational destabilizing factors.

1 INTRODUCTION

To obtain current information about the state of the high-tech complex (HTC), as an object of control of a complex technical system, the information-measuring system (IMS) must perceive the measured input values and convert them into signals necessary for: formation and implementation of norms in analog and digital types; comparison of values of input signals or functions from them with norms (settings); formation of quantitative judgment and its issuance in the information model and/or in the circuit of the automated control system (ACS) [25]. And some studies prove that the use of non-classical theory of measurement errors for processing time series allows to detect the presence of weak, not removed from the processing of sources of systematic errors [15].

On the other hand, the aerohydrodynamic and climatic conditions of HTC operation and the aggressive impact of the marine environment significantly reduce the resource of HTC. This feature requires the use of methods for forecasting the technical condition of HTC in order to assess the possible time of its safe operation [7]. The specificity of the problem is mainly in the assessment of causal relationships between the controlled parameters of the equipment and defects that may cause their change, and the possibility of further operation of HTC [16]. The presence of errors in measuring and control devices leads to specific errors that should be taken when assessing the quality of control and solving management problems of HTC [4]. That is why the task of creating diagnostic and forecasting tools that operate in complex operating conditions and adapted for continuous, long-term and reliable monitoring of the state of HTC elements under the action of concentrated destabilizing factors is relevant and in demand.

2 PURPOSE OF WORK

Ensuring high efficiency and reliability of HTC, which is achieved by introducing new tools for diagnosing and forecasting the technical condition, increasing the adequacy of estimating the parameters of HTC elements through the use of the principles of partial invariance to external uncontrolled influences on measurements.

Achieving this goal involves solving the following tasks:
– determination of noise-resistant to the impact of operational destabilizing factors (DF) means of diagnosis and forecasting of the technical condition of the elements of HTC;
– synthesis of the model of automated diagnostics of the technical condition of HTC taking the metrological characteristics of noise-tolerant sensors.

3 CONTENTS AND RESULTS OF THE RESEARCH

The analysis of the known solutions proves that for modern technical operation of HTC the newest means of diagnosing and forecasting of a technical condition are demanded, namely: devices of fiber optics insensitive to the majority of operational DF [22]. Most scientific research does not define the methods of construction, principles and features of synthesis of diagnostic and technical condition of equipment operated under the influence of concentrated DF, does not consider structural and technological features of construction and synthesis of such tools, does not assess the stability of their characteristics in difficult conditions operation [34].

On the other hand, using large data from IMSs and current forecast data corresponding to time-dependent operational situations and hydrometeorological conditions, respectively, models for detecting DF based on avoidance behavior are presented to identify potential DF scenarios [28]. Research shows that DF risk assessments can be extremely diverse depending on the operational regime, and in 97.5% of potential scenarios, warning actions are triggered only when the risk is 45% or more of its maximum value [29]. At present, these scenarios are not taken in databases of such cases, determining outside the agreed risk criteria for the operation of protection and assessing the nature of the risk during the operational mode [11].

During the operation of HTC it should be borne in mind that the change in the geometry of the controlled elements due to wear occurs in the case of frictional contact of parts [18]. Therefore, determining the amount of wear is a necessary prerequisite for the safe operation of HTC. As a rule, the sensitive elements of measuring devices are built into the elements whose technical condition is controlled [10].

Comparative analysis of fiber-optic wear sensors showed that in most cases, there are practical implementations of sensors based on Bragg fiber lattice [1]. Also known is the circuit design of the wear sensor, which consists of a fiber with a Bragg fiber lattice, which is built perpendicular to the wear surface (Fig. 1).
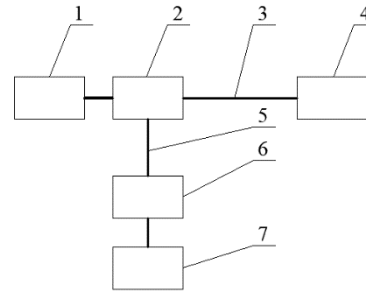
Figure 1. Block diagram of the measuring system of the wear sensor with Bragg fiber lattice: 1 – radiation source; 2 – splitter; 3 – primary fiber; 4 – fiber with a Bragg lattice that is in contact with the tribo-surface; 5 – secondary fiber; 6 – photodetector; 7 – controller for determining the amount of wear

In addition to the wear of parts of the elements of the HTC, it is necessary to take the peak loads (twisting) on the shafts, which can lead to their physical destruction. Assuming that the measured load x and the measurement error in the probabilistic sense are independent, the control result can be obtained by operating with the composition of the distribution density $F(x)$ and $\theta(\varepsilon)$, Fig. 2, a, b.

For practical purposes, it is of interest to use approximate estimates of these probabilities, for example, using nomograms linking the standard deviation of the error of the measuring devices σ_ε and the controlled value σ_x, as well as the tolerance zone r. Error reduction can be achieved by repeating control operations repeatedly or by double-checking, using, taking the required accuracy, different control systems [30].

At the same time, it is known that friction in the tribo-combination depends on the microrelief of the surface and is a source of vibration of the high frequency range, the presence of which requires appropriate measures for their filtration at the level of power sources IMS. Wear sensors focused on controlling the vibration of the surfaces to be worn consist of a sealed housing with the base and the light guide with a cantilever-mounted mirror (Fig. 3) [21].

In the process of measurement and control there is a problem of sampling of one or another controlled quantity, i.e. the task of determining the allowable value of the control interval. Assume that at time ti the operation of load control HTC is performed and it is established that it is in the zone {PH, PD} (Fig. 2). In this case, the estimation of the control result can be the probability $p\ (x \in r)$ that at $t_{i+1} = t_i + \varDelta t$ the load will not go beyond {PH, PD}, i.e. the conditions will be met [26]:

$$x_{PD} \le x(t_i + \Delta t) \le x_{PH} \tag{1}$$

were $x(t_i + \varDelta t) = \dot{x}(t_i)\varDelta t$ and $\dot{x}(t_i)$ – derivative.
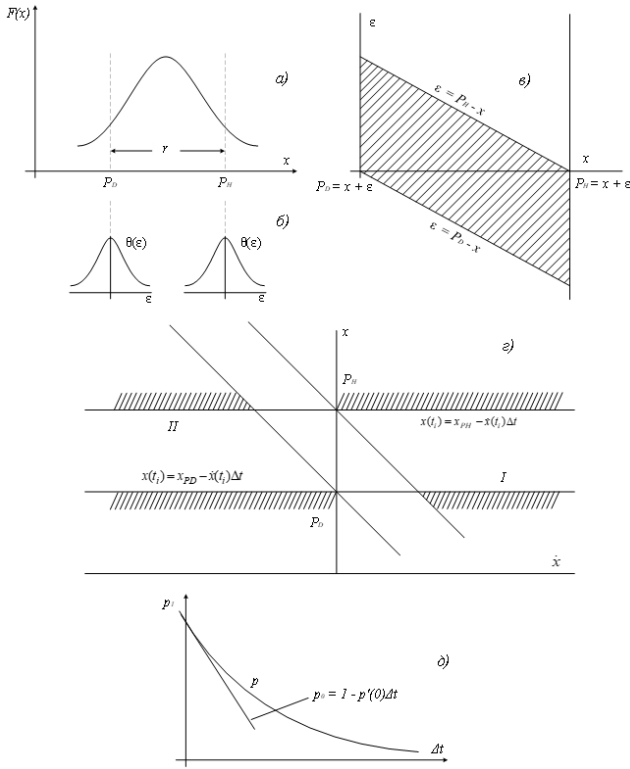
Figure 2. Distribution densities: a) probability distribution density of the controlled variable $F(x)$; b) the density of the error probability distribution $\theta(\varepsilon)$; c) the composition $F(x)$ and $\theta(\varepsilon)$; d) the composition $f_1(x)$ and $f_2(x)$; e) the graph explaining the process of determining the probabilities $p_0(\delta)$
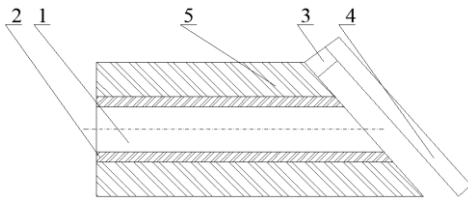
Figure 3. Vibration wear sensor: 1 – optical fiber; 2 – shell; 3 – console support; 4 – mirror; 5 – basis

The problem of increasing the stability and reliability of measurements of precision sensors [20] by minimizing their temperature drift is solved using methods based on design and technological improvements that minimize destabilizing factors initiated by a variable intensity temperature field [31]. The most expedient and economically justified is the way to improve fiber-optic wear sensors, based on the use of passive methods to minimize temperature drift in the most thermostable known circuit solutions [2].

In [9] it is proposed to use as a material that provides the necessary mechanical characteristics of the oscillating system for the control of the elements of rotary machines of fibers based on artificial sapphire. It is investigated that the use of single-mode optical fibers made [33] of artificial sapphire with a depressed core and a wavelength of 1.55 μm will increase not only the resistance of the sensor elements to DF, but also increase the relative amount of radiation power (Fig. 4).

Changing the linear dimensions of the sensor base at elevated temperatures up to 250° can reach $1{,}25 \cdot 10^{-5}$ m. Thermo-deformation of the biscle plate, when connected with its base and secondary fiber

(Fig. 5), will create an axial shift of the latter in the direction of the primary fiber [24].
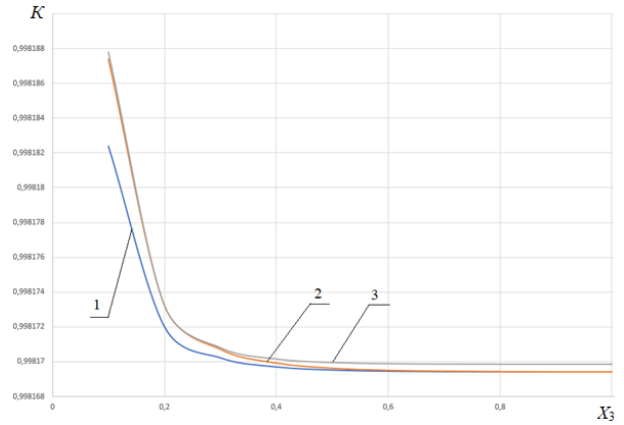
Figure 4. The relative intensity K depending on the gap x_s between the primary and secondary fibers of artificial sapphire for different wavelengths of optical radiation λ, μm: 1 – 0.85; 2 – 1.33; 3 – 1.55
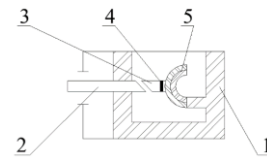
Figure 5. Fiber-optic vibration sensor wear: 1 – base; 2 – primary fiber; 3 – secondary fiber; 4 – reflective layer; 5 – braided console plate

The following initial data were used to estimate the value of possible compensation of thermal propagation of sensor elements due to the use of the plate: material of primary and secondary fibers – artificial sapphire with refractive indices (RI) $n = 1.75$; base material quartz glass with software $n = 1.48$; the composition of the glass plate – glass made of artificial sapphire with a coefficient of thermal linear expansion $\alpha_1 = 5{,}6 \cdot 10^{-6}$ and glass brand KRS5 with $\alpha_1 = 5{,}8 \cdot 10^{-5}$; the thickness of the glass plate $\Delta h = 5 \cdot 10^{-4}$ m; temperature range $\Delta T = 50 \ldots 250$ °C; due to the bending of the glass plate and the thermal propagation of the base [3].

Based on these limitations, it is possible to determine the relative intensity depending on the gap:

$$K = 1 - \left[\left(z^2 + \gamma^2 \right)^2 \left[\left(z^2 + \gamma^2 \right)^2 + 4z^2\gamma^2 \coth^2\left(\frac{\beta}{2} \right) \right]^{-1} \right], \qquad (2)$$

where

$$\beta = \left(\frac{4\pi x}{\lambda} \right)\left(n^2 \sin^2 \Theta - 1 \right)^{0,5}$$

for radiation polarized perpendicular to the plane of incidence

$$Z = \frac{1}{n\cos\Theta}, \quad \gamma = -\left(n^2 \sin^2 \Theta - 1 \right)^{-0,5};$$

for radiation polarized in the plane of incidence

$$Z = \frac{\cos \Theta}{n}, \quad \gamma = -\left(n^2 \sin^2 \Theta - 1\right)^{0,5} \tag{3}$$

$$x = x_3 + \Delta x = x_3 + \left(\frac{l_0^2\left(\alpha_2 - \alpha_1\right)\Delta T \Delta h}{8 \Delta h} - l_0\left(1 + \alpha \Delta T\right)\right).$$

If the calculations take the average value for both possible polarizations, then when using a glass plate, the addition of the value of K in the temperature range $\Delta T = 50\ldots250°C$ will be within $6\ldots9{,}5\cdot10^{-3}$ %. This value of the application of the coefficient of relative intensity can be neglected.

If we limit the measurement error $x_{PH} - x_{PD} > \varepsilon_{max}$ and use the conclusions [23], we can find the probability of error of the first MIS (1) and the second MIS (2) kind:

$$\text{MIS(1)} = \int_{PD(l)}^{PH(l)} F(x) \left(\int_{-\infty}^{x_{PD}-x} \theta(\varepsilon)d\varepsilon + \int_{x_{PH}-x}^{\infty} \theta(\varepsilon)d\varepsilon \right) dx;$$

$$\text{MIS(2)} = \int_{-\infty}^{PD} F(x) \left(\int_{x_{PD}-x}^{x_{PH}-x} \theta(\varepsilon)d\varepsilon \right) dx + \int_{PH}^{\infty} f(x) \left(\int_{x_{PD}-x}^{x_{PH}-x} \theta(\varepsilon)d\varepsilon \right) dx;$$

The probability $p(x(t_i + \Delta t))$ depends on the width of the interval r, the dynamic properties of the load and the value of $x(t_i)$. It can be found by integrating the conditional density $f(x, \dot{x}/x_{PD}) < x < x_{PH}$ in regions I and II (Fig. 2, c). Assuming that the distribution $\dot{x}$ (3) is also normal, then

$$f(x, \dot{x}) = f_1(x) f_2(x) \tag{4}$$

where

$$f_1(x) = \frac{1}{p\sqrt{2\pi}\sigma_x} \exp\left(-\frac{\left(x - M_x^2\right)}{2\sigma_x^2}\right);$$

$$f_2(x) = \frac{1}{\sqrt{2\pi}\sigma_{\dot{x}}} \exp\left(-\frac{\dot{x}^2}{2\sigma_x^2}\right)$$

Probability $(1 - p)$ can be found as

$$1 - p = \int^{(x_{PH}-x_{PD})/\Delta t} f_2(\dot{x})d\dot{x} \int_{x_{PH}-\dot{x}\Delta t}^{x_{PH}} f_1(x/x_{PD}, x_{PH})dx +$$

$$+ \int_{(x_{PH}-x_{PD})/\Delta t}^{\infty} f_2(\dot{x})d\dot{x} \int_{x_{PD}}^{x_{PH}} f_1(x/x_{PH}, x_{PD})dx +$$

$$+ \int^{(x_{PD}-x_{PH})\Delta t} f_2(\dot{x})d\dot{x} \int_{x_{PD}}^{x_{PH}} f_1(x/x_{PD}, x_{PH})dx.$$

At small Δt (see Fig. 2, d), the probability p will be equal

$$p_0 = 1 - \Delta t\left(dp / d\left(\Delta t\right)\right)\Delta t = 0$$

From here $\Delta t = \frac{t - p_0}{\left(dp / d\left(\Delta t\right)\right)\Delta t}$. Differentiating the expression $(1 - p)$ by Δt and substituting it in the expression for Δt, you can get the allowable value of the control interval:

$$\Delta t_{ad} = \frac{p(1 - p_0^*)}{\frac{\sigma_{\dot{x}}}{2\pi\sigma_x}\left(\exp\left(-(x_{PH} - M_x)^2 / 2\sigma_x^2\right) + \exp\left(-(x_{PD} - M_x)^2 / 2\sigma_x^2\right)\right)},$$

where p and p_0^* – apriority and given probabilities of finding the controlled size of loading.

To simplify the determination of the control interval with a known maximum error ε_{max} and the maximum modulus of the first derivative of the controlled load, you can use the expression:

$$\Delta t = \varepsilon_{max} / \Delta t\left(dx(t) / dt\right)_{max},$$

and thus take $\varepsilon_{max} = 3\sigma_\varepsilon$, and $(dx(t)/dt)_{max}$ determine by conducting an appropriate analysis of the function $f(\dot{x})$.

Further consideration will be given only for emissions for the upper level of the load HTC [12]. The most important issues are to determine the law of distribution of the time of the random function above a given level and the law of distribution of the number of emissions [17].

The load output beyond the upper limit is described by the inequalities $x(t) + \dot{x}(t)dt > x_{PH}$ or $x_{PH} - \dot{x}(t)dt < x(t) < x_{PH}$, and the probability of EPH emission will be determined by the expression

$$E_{PH}(x_{PH} - \dot{x}(t)dt < x(t) < x_{PH}) = \int_0^{\infty} \int_{x_{PH}-\dot{x}dt}^{x_{PH}} f(x(t), \dot{x}(t))dxd\dot{x} \tag{5}$$

Since $\dot{x}dt \ll x_{PH}$, i.e. the limits of integration differ little, and also assuming that the emission probability is proportional to the value of the time interval [19], simplify expression (5) and introduce the concept of time density for the emission probability $l_{PH}\left(x_{PH} / t\right)$:

$$l_{PH}(x_{PH} / t) = \int_0^{\infty} f(x_{PH}, \dot{x} / t)dxd\dot{x};$$

$$l_{PD}(x_{PD} / t) = \int_0^{\infty} f(x_{PD}, \dot{x} / t)dxd\dot{x}, \tag{6}$$

where $f(\dot{x}/t)$ – conditional density distribution of the value of $\dot{x}$ over time.

In this case, the average residence time of the load above the specified limit for the period of time T will be found as

$$T_{\Sigma PH, PD} = \int_0^T \int_{x_{PH}}^{\infty} f(x / t)dxdt, \tag{7}$$

and the average duration of the single emission [14] (from the practical point of view, this is the most important characteristic):

$$\overline{\tau}_{PH} = \frac{\overline{T}_{\Sigma PH}}{N_{PH}} = \frac{\int\limits_0^T \int\limits_{x_{PH}}^{\infty} f(x/t)dxdt)}{\int\limits_0^T \int\limits_0^{\infty} f(x_{PH}, dx/t)d\dot{x}dt} \qquad (8)$$

If we now assume that the conditional density of the ordinate distribution of the random function $f(x/t)$ and the function $f(dx/t)$ does not depend on time, then the search task is greatly simplified [13]. In this case, similarly to (4), the distribution laws $f(x)$ and $f(x, \dot{x})$ are uniquely expressed through the mathematical expectation M_x and the variance σ_x and $\sigma_{\dot{x}}$, since the mathematical expectation of the derivative $M_{\dot{x}}$ due to the stationaryness of the random process is zero.

The variance σ_x^2 is determined by the correlation function of the velocity at zero ($\tau = 0$):

$$\sigma_x^2 = -\frac{d^2 K_x(r)}{d\tau^2} \Big| \tau = 0 \cdot$$

As a result of conversions we will receive:

$$T'_{\Sigma PH} = T \int\limits_{x_{PH}}^{\infty} f(x)dx; \qquad N'_{PH} = T \int\limits_0^{\infty} dxf(x,\dot{x})d\dot{x};$$

$$\overline{\tau}'_{PH} = \frac{\int\limits_{x_{PH}}^{\infty} f(x)dx}{\int\limits_0^{\infty} dxf(x,\dot{x})dx}; \qquad (9)$$

$$\nu_{PH} = \frac{N'_{PH}}{T} = \frac{\sigma_{\dot{x}}}{2\pi\sigma_x} \exp\left(-\frac{(x_{PH} - M_x)}{2\sigma_x^2}\right); \qquad (10)$$

$$\tau'_{PH} = \pi \frac{\sigma_x}{\sigma_{\dot{x}}} \exp\left(-\frac{(x_{PH} - M_x)}{2\sigma_x^2}\right)\left(1 - \Phi\left(\frac{x_{PH} - M_x}{\sigma_x}\right)\right),$$

where $\Phi(z) = \Phi(M_x, \sigma_x, x_{PH})$ – Laplace function:

$$\Phi(z) = \frac{1}{\sqrt{2\pi}} \int\limits_0^z e^{-x^2/2} dx, z = \frac{x_{PH} - M_x}{\sigma_x}.$$

It should be noted that, using the tables of Laplace functions $\Phi(z)$, for example [27], it is possible to calculate the probability of feedback of the predicted load $x \in N(M_x, \sigma_x)$ in the interval x_{PH}, x_{PD}. To do this, you must first calculate $z_1 = \frac{x_{PD} - M_x}{\sigma_x}$ and $z_2 = \frac{x_{PH} - M_x}{\sigma_x}$, and then, using Laplace [5] tables to find $\Phi(z_1)$ and $\Phi(z_2)$. In this case, the probability is defined as

$$p(x_{PD} < x < x_{PH}) = \Phi(z_2) - \Phi(z_1). \qquad (11)$$

When determining the control processes of HTC with the use of electricity storage, you need to forecast the value of energy required to ensure the emission of the load above a given level. It is clear that in this case the average area $\overline{S}$ limited by the implementation of the normal and stationary random function above a given level of x_{PH} at the time of release, and therefore determined:

$$\overline{S} = \frac{\sigma_x^2 \sqrt{2\pi}}{\sigma_{\dot{x}}} + \frac{(\overline{x} - x_{PH})\sigma_x \pi}{\sigma_{\dot{x}}} \times$$
$$\times \left(1 - \Phi\left(\frac{x_{PH} - \overline{x}}{\sigma_x}\right)\exp\left(-\frac{(x_{PH} - \overline{x})^2}{2\sigma_x^2}\right)\right). \qquad (12)$$

Let us also determine the request for estimating the global mathematical expectation M_x load on the considered interval, which is stored in the computer memory and should be periodically adjusted (if required by the evaluation results). For this purpose, we use the Monte Carlo method [8]. In this case, the computer memory must have the average of the sample value x load for the last $N > 10$ observations. Assuming that the distribution of random values $\overline{x}$ is asymptotically normal and taking the well-known rule of "three sigmas" [32]:

$$P(|M_x - \overline{x}| < 3\frac{\sigma_x}{\sqrt{N}}) \approx 2\Phi_0(3) \approx 0,997,$$

we formulate the conditions for the need to correct the global mathematical expectation in the form of a predicate Π_{MX}:

$$\forall M_x \forall \overline{x} \forall \sigma_x \forall N\left(|M_x - x| > 3\frac{\sigma_x}{\sqrt{N}}\right) \to \Pi_{MX}\left(M_x, x, \sigma_x, N\right), \qquad (13)$$

where

$$\sigma_x \approx \left(\frac{1}{N-1}\sum_{i=1}^N (x_i - \overline{x})^2\right)^{1/2}.$$

Then we find the static estimate of the constant mathematical expectation [6] by averaging:

$$m_x^* = \frac{1}{T}\int\limits_0^T x(t)dt \qquad (14)$$

and to determine the estimate of the correlation function we use known formulas:

$$K_x^*(t) = \frac{1}{T-\tau}\int\limits_0^{T-\tau}\left(x(t) - m^*(x)\right)(x(t+\tau) - m_x^*)dx;$$
$$K_x^*(t) = \frac{1}{m-n-1}\sum_{i=1}^{m-n}(x(t_i) - \overline{x})(x(t_i + \tau) - \overline{x}), \qquad (15)$$

where m – is the number of quantization intervals on the entire interval T, and n is the number of quantization intervals on the interval τ.

4 CONCLUSIONS AND RECOMMENDATIONS

The proposed tool for diagnosing the operation of HTC is invariant to external uncontrolled influences on diagnostic processes, which allows for continuous monitoring, preventive diagnosis of the technical condition of the elements of VTK, improve the quality of their technical operation and repair. We emphasize that formulas (14) and (15) are valid in assuming the ergodicity of the process, which can be judged by the behavior of its correlation function. Thus, if $K_x(\tau)$

converges to zero on the finite interval τ, then this fact serves as a sufficient condition for the ergodicity of the process itself $x(t)$ (see Fig. 7, b), because $\left|K_x(\tau)\right| \leq 0,05$. In Figs. 7, 8 and 9 show the results of statistical processing of experimental studies of HTC for different types of vessels.
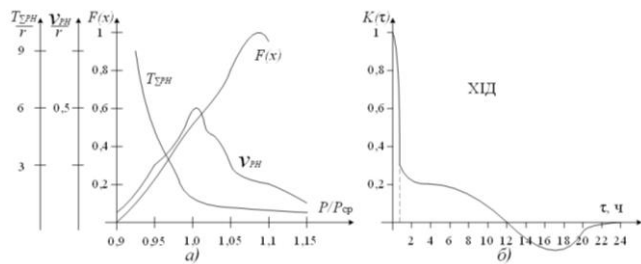
Figure 7. The results of experimental evaluation load characteristics (a) and the normalized correlation function, designed for many implementations (b)

It is determined that the introduction of a new means of preventive diagnosis of the technical condition of tribodes will increase the efficiency of use and reliability of HTC by reducing the accident rate ~10 %, increasing the maintenance period and reducing operating costs with an average load.
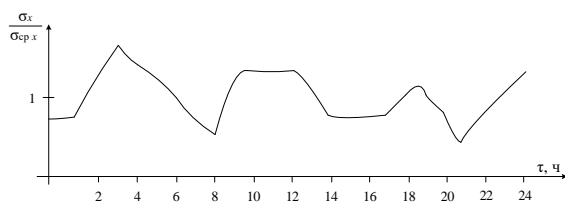
Figure 8. Daily changes in mathematical expectations relative to the average values
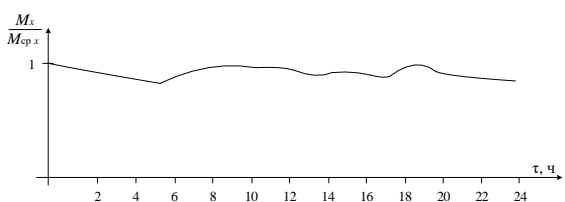
Figure 9. Daily changes in standard deviation relative to average values

Errors of the first and second kind are distinguished, the probability of false indication and omission of registration of transition of parameters X of limit value, accordingly, is estimated. The measured parameters X are connected with the generated power in the running mode of l-parallel generating sets, the change of which should be controlled between the upper X_{PH} and lower X_{PD} loading thresholds.

REFERENCES

1. Akand, T. et al.: Low loss hollow-core optical fibers conjoining tube lattice and revolver structures. Results in Optics. 1, 100008 (2020). https://doi.org/10.1016/j.rio.2020.100008.
2. Akrofi, J.D. et al.: Multi-stack insulator to minimise threshold voltage drift in ZnO FET sensors operating in ionic solutions. Micro and Nano Engineering. 8, 100066 (2020). https://doi.org/10.1016/j.mne.2020.100066.
3. Allam, A. et al.: Linear Thermal Expansion Coefficients of Higher Manganese Silicide Compounds. Physics Procedia. 55, 24–29 (2014). https://doi.org/10.1016/j.phpro.2014.07.004.
4. Barde, M., Barde, P.: What to use to express the variability of data: Standard deviation or standard error of mean? Perspect Clin Res. 3, 3, 113–116 (2012). https://doi.org/10.4103/2229-3485.100662.
5. Bourne, M.: Table of Laplace Transforms, https://www.intmath.com/laplace-transformation/table-laplace-transforms.php, last accessed 2022/03/30.
6. Budashko, V. et al.: Conceptualization of research of power hybrid electric power complexes. TAPR. 5, 1(31), 63–73 (2016). https://doi.org/10.15587/2312-8372.2016.81407.
7. Budashko, V.: Design of the Three-Level Multicriterial Strategy of Hybrid Marine Power Plant Control for a Combined Propulsion Complex. Electrical engineering & electromechanics. 2, 62–72 (2017). https://doi.org/10.20998/2074-272X.2017.2.10.
8. Budashko, V.: Formalization of design for physical model of the azimuth thruster with two degrees of freedom by computational fluid dynamics methods. EEJET. 3, 7 (87), 40–49 (2017). https://doi.org/10.15587/1729-4061.2017.101298.
9. Budashko, V.: Theoretical-Applied Aspects of the Composition of Regression Models for Combined Propulsion Complexes Based on Data of Experimental Research. Eastern-European Journal of Enterprise Technologies. 3, 88, 11–20 (2017). https://doi.org/10.15587/1729-4061.2017.107244.
10. Budashko, V., Shevchenko, V.: Solving a Task of Coordinated Control Over a Ship Automated Electric Power System under a Changing Load. Eastern-European Journal of Enterprise Technologies. 2, 110, 54–70 (2021). https://doi.org/10.15587/1729-4061.2021.229033.
11. Budashko, V., Shevchenko, V.: The Synthesis of Control System to Synchronize Ship Generator Assemblies. Eastern-European Journal of Enterprise Technologies. 2, 109, 45–63 (2021). https://doi.org/10.15587/1729-4061.2021.225517.
12. Budashko, V.V.: Increasing Control's Efficiency for the Ship's Two-mass Electric Drive. Electrical Engineering & Electromechanics. 0, 4, 34–42 (2016). https://doi.org/10.20998/2074-272X.2016.4.05.
13. Chen, B., Luo, X.-L.: Novel multivariate q-sigma rule focusing on process variation for incipient fault detection in dynamic processes. Chemometrics and Intelligent Laboratory Systems. 206, 104149 (2020). https://doi.org/10.1016/j.chemolab.2020.104149.
14. Dunn, W.L., Shultis, J.K. eds: Exploring Monte Carlo Methods. Elsevier, Amsterdam (2012). https://doi.org/10.1016/B978-0-444-51575-9.00017-8.
15. Dvulit, P. et al.: Accuracy estimation of site coordinates derived from GNSS-observations by non-classical error theory of measurements. Geodesy and Geodynamics. 12, 5, 347–355 (2021). https://doi.org/10.1016/j.geog.2021.07.005.
16. Fonseca, T. et al.: Assessing innovation in transport: An application of the Technology Adoption (TechAdo) model to Maritime Autonomous Surface Ships (MASS). Transport Policy. 114, 182–195 (2021). https://doi.org/10.1016/j.tranpol.2021.09.005.
17. den Hollander, F. et al.: Law of large numbers for non-elliptic random walks in dynamic random environments. Stochastic Processes and their Applications. 123, 1, 156–190 (2013). https://doi.org/10.1016/j.spa.2012.09.002.

18. Holmberg, K. et al.: Topography orientation effects on friction and wear in sliding DLC and steel contacts, part 3: Experiments under dry and lubricated conditions. Wear. 486–487, 204093 (2021). https://doi.org/10.1016/j.wear.2021.204093.

19. I. Hvozdeva et al.: Problems of Improving the Diagnostic Systems of Marine Diesel Generator Sets. In: 2020 IEEE 15th International Conference on Advanced Trends in Radioelectronics, Telecommunications and Computer Engineering (TCSET). pp. 350–354 (2020). https://doi.org/10.1109/TCSET49122.2020.235453.

20. Kakinuma, Y. et al.: External Sensor-less On-machine Measurement of Workpiece for Ultra-precision Machine Tools. Procedia CIRP. 9, 40–43 (2013). https://doi.org/10.1016/j.procir.2013.06.165.

21. Khonsari, M.M. et al.: On the running-in nature of metallic tribo-components: A review. Wear. 474–475, 203871 (2021). https://doi.org/10.1016/j.wear.2021.203871.

22. Krčum, M. et al.: Shipboard Monitoring and Control System. IFAC Proceedings Volumes. 30, 22, 165–169 (1997). https://doi.org/10.1016/S1474-6670(17)46508-6.

23. Lee, C., Kim, J.: Energy Efficient Control for Electric Ship Propulsion Considering Thrust Fluctuation in Regular Waves. IFAC-PapersOnLine. 54, 16, 364–369 (2021). https://doi.org/10.1016/j.ifacol.2021.10.117.

24. Mehnert, M. et al.: A complete thermo–electro–viscoelastic characterization of dielectric elastomers, Part I: Experimental investigations. Journal of the Mechanics and Physics of Solids. 157, 104603 (2021). https://doi.org/10.1016/j.jmps.2021.104603.

25. Rethfeldt, C. et al.: System Approach for Highly Automated Manoeuvring with Research Vessel DENEB. IFAC-PapersOnLine. 54, 16, 153–160 (2021). https://doi.org/10.1016/j.ifacol.2021.10.087.

26. Tang, R. et al.: Optimal operation of hybrid energy system for intelligent ship: An ultrahigh-dimensional model and control method. Energy. 211, 119077 (2020). https://doi.org/10.1016/j.energy.2020.119077.

27. Tillmann, A.M., Kobbelt, L.: Structured discrete shape approximation: Theoretical complexity and practical algorithm. Computational Geometry. 99, 101795 (2021). https://doi.org/10.1016/j.comgeo.2021.101795.

28. V. Budashko: Thrusters Physical Model Formalization with regard to Situational and Identification Factors of Motion Modes. In: 2020 International Conference on Electrical, Communication, and Computer Engineering (ICECCE). pp. 1–6 (2020). https://doi.org/10.1109/ICECCE49384.2020.9179301.

29. V. Myrhorod et al.: Multi-parameter Diagnostic Model of the Technical Conditions Changes of Ship Diesel Generator Sets. In: 2020 IEEE Problems of Automated Electrodrive. Theory and Practice (PAEP). pp. 1–4 (2020). https://doi.org/10.1109/PAEP49887.2020.9240905.

30. Wang, P. et al.: Effects of bipolar repetitive square wave voltage parameters on electrical tree characteristics of epoxy resin. Polymer Testing. 103, 107371 (2021). https://doi.org/10.1016/j.polymertesting.2021.107371.

31. Wang, S. et al.: High-precision fiber optic liquid level sensor based on fast Fourier amplitude demodulation in a specific range of spectrum. Measurement. 187, 110326 (2022). https://doi.org/10.1016/j.measurement.2021.110326.

32. Wang, X. et al.: Random fiber laser based on an artificially controlled backscattering Erbium-Doped fiber. Optical Fiber Technology. 54, 102125 (2020). https://doi.org/10.1016/j.yofte.2019.102125.

33. Wang, Y.-Y. et al.: Real-time monitoring of pressure and temperature of oil well using a carbon-coated and bellow-packaged optical fiber sensor. Optical Fiber Technology. 67, 102703 (2021). https://doi.org/10.1016/j.yofte.2021.102703.

34. Zhang, M. et al.: A Big Data Analytics Method for the Evaluation of Ship - Ship Collision Risk reflecting Hydrometeorological Conditions. Reliability Engineering & System Safety. 213, 107674 (2021). https://doi.org/10.1016/j.ress.2021.107674.